

# Shadow brightness and shadow fraction relations with effective leaf area index: importance of canopy closure and view angle in mixedwood boreal forest

Evan D. Seed and Douglas J. King

**Abstract.** This research examines the impacts of varying canopy closure and view angle on relations of high-resolution digital camera shadow fraction and shadow brightness with mixedwood boreal forest effective leaf area index (LAI<sub>e</sub>). Results from linear regression analyses revealed weak and insignificant positive relations between shadow fraction and LAI<sub>e</sub>. Considerable scatter was observed in the relationship and was attributed to differences in canopy closure among plots, as only forest with greater than 80% closure showed a positive relationship between shadow fraction and LAI<sub>e</sub>. These results emphasized that gap size and frequency were important factors in determining the shadow fraction. Relations between shadow brightness and LAI<sub>e</sub> were significantly improved over those with the shadow fraction because of decreased data point scatter when closure was less than 80%. Shadow brightness was not adversely affected by canopy closure, while remaining sensitive to species composition. The association of shadow fraction with LAI<sub>e</sub> was understood to exist through links to the projected shadow area of tree crowns; however, this relation became unstable in more open canopies. With shadow brightness, surrogate information on LAI<sub>e</sub> was implicitly linked to differences in the transmission of light through deciduous and coniferous tree crowns. An evaluation of view angle geometry effects suggested that bidirectional reflectance impacts on the shadow fraction – LAI<sub>e</sub> relations were strongest in the forward-scattering direction, but had less effect on regression analysis in the backscattering direction and at nadir.

**Résumé.** Cette étude examine les impacts de la variation de la fermeture du couvert et de l'angle de visée sur les relations entre les fractions d'ombre et l'intensité de l'ombre obtenues à l'aide d'une caméra numérique à haute résolution et les valeurs de LAI<sub>e</sub> de secteurs de forêt mixte en forêt boréale. Les résultats des analyses de régression linéaire ont révélé des relations positives faibles et non significatives entre les fractions d'ombre et le LAI<sub>e</sub>. Une dispersion importante a été observée dans la relation et celle-ci a été attribuée à des différences dans la fermeture du couvert au sein des parcelles, étant donné que les forêts présentant des taux de fermeture supérieurs à 80 % affichaient une tendance positive avec le LAI<sub>e</sub>. Ces résultats indiquent que la taille et la fréquence des trouées constituaient des facteurs importants dans la détermination des fractions d'ombre. Les relations entre l'intensité de l'ombre et le LAI<sub>e</sub> dénotent une amélioration significative par rapport aux fractions d'ombre en raison de la réduction de la dispersion des points de données lorsque le taux de fermeture est de moins de 80 %. L'intensité de l'ombre n'est pas affectée négativement par la fermeture du couvert, tout en demeurant sensible à la composition des espèces. L'existence de l'association entre les fractions d'ombre et le LAI<sub>e</sub> est démontrée par le biais de liens par rapport à la zone d'ombre projetée des couronnes d'arbres. Toutefois, cette relation devient instable dans les couverts plus ouverts. Avec l'intensité de l'ombre, l'information de substitution sur le LAI<sub>e</sub> est implicitement reliée aux différences observées dans la transmission de la lumière à travers les couronnes des feuillus et des conifères. Une évaluation des effets de la géométrie de l'angle de visée permet de croire que les impacts de la réflectance bidirectionnelle sur les relations ombres-LAI<sub>e</sub> sont plus forts dans la direction de la diffusion avant, mais qu'ils ont moins d'effet sur l'analyse de régression dans la direction de la rétrodiffusion et au nadir.

[Traduit par la Rédaction]

## Introduction

This paper addresses one of the key challenges to applying remote sensing for the estimation of leaf area index (LAI) in the boreal forest, that is, to develop reliable and efficient methods for use in mixedwood forest. Defined by Chen and Cihlar (1996) as half the total (all-sided) leaf area per unit ground surface area, LAI is a quantitative measure of canopy structure that accounts for the nonrandom or clumped nature of forest structural elements at the leaf, shoot, and branch levels (Chen and Cihlar, 1995). Similar to LAI, effective leaf area index

(LAI<sub>e</sub>) is also a measure of forest canopy structure; however, it corresponds to estimates of LAI obtained by inversion from the canopy gap fraction assuming randomly distributed leaves, shoots, and branches. It is often associated with LAI as viewed and measured by optical instruments such as the LAI-2000

---

Received 27 April 2002. Accepted 29 January 2003.

**E.D. Seed and D.J. King.**<sup>1</sup> Department of Geography and Environmental Studies, Carleton University, 1125 Colonel By Drive, Ottawa, ON K1S 5B6, Canada.

<sup>1</sup>Corresponding author (e-mail: doug\_king@carleton.ca).

plant canopy analyzer (LI-COR, Inc., Lincoln, Nebr.). Although LAI<sub>c</sub> is the focus of research presented in this paper, background material is placed in the broader context of LAI for general discussion purposes.

From an image-analysis perspective, mixedwood forest presents a much different scenario for LAI retrieval than single-species forest where extraction of information can be stratified a priori according to cover type (Peddle et al., 1997). Subtle differences in topography, soil moisture, drainage, and stand management practices can often produce a complex mosaic of forest cover types at local and regional scales. In many forested regions it is typical for conifer and deciduous species to occur together during various stages of stand development and replacement, resulting in mixedwood stands (Kneeshaw and Bergeron, 1998; Bonan and Shugart, 1989). In these stands, even when species composition is known, it may not be possible to stratify the forest into homogeneous units based on cover type if there are no clear means of delineating forest with a conifer-dominated canopy from that with a deciduous-dominated canopy. This is especially difficult in stands that vary in composition at scales finer than those of the auxiliary data typically used to provide the information on species composition (Jones et al., 1983). The primary question that must be addressed in developing models for mixedwood LAI estimation centres on how best to measure and extract image variance that maximizes information on forest overstory LAI. This means extracting information that is representative of an assemblage of species and forest structures that control the variation of tone in the image. For these reasons, any empirical model must be applicable to a range of crown geometries in the overstory and, in addition, often account for uncertainties in the remote sensing signal from understory layers characteristically present in stands with low to medium closure (Spanner et al., 1990; Chen and Cihlar, 1996). As suggested by Wulder et al. (1998), Brown et al. (2000), and Chen et al. (1999), there is a need and potential for development of species-independent models for estimating boreal forest LAI.

Image radiometric structure analysis is one method that holds promise as an operational alternative to traditional vegetation indices for estimating LAI in the boreal forest (Hall et al., 1995; Peddle and Johnson, 2000; Peddle et al., 2001). Driven by the theory of geometric-optical models (Li and Strahler, 1985; Rosema et al., 1992; Gastellu-Etchegorry, 1996; Gerard and North, 1997; Chen and Leblanc, 1997), which aid in image understanding, image structure analysis techniques such as spectral mixture analysis provide a physical link between the canopy and image by explicitly treating canopy geometry in the image as a series of discrete objects (trees) that are capable of casting shadows between and within individual crowns (Chen and Leblanc, 1997). With this approach, the fundamental structure of an image is defined by the radiometric components of (i) sunlit background, (ii) sunlit canopy, (iii) shaded canopy, and (iv) shaded background, or simply by sunlit and shadow components. Here, methods are termed structural in the sense that image primitives are explicitly defined as regions of pixels, that is, in contrast to techniques such as image grey level co-

occurrence texture (Haralick et al., 1973) where the image primitive is defined as a single pixel. In particular, studies using radiometric component analysis have shown a strong positive relationship between the image shadow fraction and LAI in homogeneous spruce and aspen stands using both satellite and airborne imagery. Unlike vegetation indices, the shadow fraction tends to remain sensitive to increases in stand LAI above 4 and more robust under a variety of stand densities (Peddle et al., 1995). Indeed, the influence of shadow on the image scene has been widely cited in remote sensing (Leblon et al., 1996; Ekstrand, 1994; Danson and Curran, 1993; Franklin et al., 1991; Ranson and Daughtry, 1987), but the results of Hall et al. (1995) and Peddle et al. (1995) were among the first to empirically exploit the relationship between object structure and shadow characteristics for the estimation of forest canopy structure. This method offers improvement over vegetation indices because it explicitly accounts for the complex three-dimensional shadow casting structure of forest canopies and is sensitive to tree size and morphology (Peddle et al., 1995; 2001). As such, these strong relations warrant the investigation of the relation between shadow fraction and LAI in additional forest cover types such as boreal mixedwood forest.

Use of the shadow fraction (area) is, however, only one of several potential shadow component attributes that can be measured. Others include spatial measures of shape, perimeter, adjacency, or co-occurrence and statistical measures such as variance, standard deviation, and mean brightness. We reason that one of these measures, shadow component brightness, may also be related to LAI through direct association with the overstory light transmission qualities of deciduous and conifer tree crowns. Because trees support leaf area, they intercept light and thus affect the light regime beneath the forest canopy, setting up a physical link between LAI and light transmission through the tree crown. Shadow component brightness is put forward as a measure of this light regime, providing surrogate information on canopy leaf area.

In fact, research has demonstrated that the microscale geometry of trees such as branching patterns, foliage, and shoot clumping may influence canopy shadowing through links to crown architecture, crown light transmission, and absorption (Ross, 1981; Oker-Blom and Kellomaki, 1983; Rosema et al., 1992; Stenberg et al., 1994; Leblon et al., 1996; Chen and Leblanc, 1997). Individual crowns are organized into stems and branches, and their particular arrangement or architecture determines the shadow brightness that is projected onto the ground or created within individual tree crowns. Conifer and deciduous trees have very different crown structures and therefore produce shadows that are unique to each type of tree. Deciduous trees such as poplar (*Populus tremuloides*, *Populus balsamifera*) are characterized by an open crown architecture where branches and foliage are located farther from the main stem than in the more closed crown architecture common to conifer species such as spruce (*Picea mariana*, *Picea glauca*). The open crown architecture of deciduous species creates conditions that favour the creation of sunflecks or penumbra on the surface where the shadows are cast. These sunflecks have

the effect of increasing the shadow brightness by adding a mixture of sun or partially diffuse light to the projected shadow area (Leblon et al., 1996). In contrast, conifers tend to have closed crown architecture with smaller branches that are relatively dense with foliage clumped and very close to the main stem forming a conical or cylindrical shape, which tends to decrease light transmission through the crown. For example, Constabel (1995) noted that light transmission through a conifer crown could be 10–50% of that transmitted through a deciduous crown with similar stem size. Specifically, spruce–aspen mixedwood stands with a higher percent composition of shade-tolerant conifer species in the overstory were shown to transmit less light to the understory than canopies dominated by shade-intolerant species such as aspen (Constabel and Leiffers, 1996; Leiffers et al., 1999).

Lastly, observed differences in light interception by deciduous and conifer trees may also be due to macroscale crown geometry, that is, crown shape and size (Oker-Blom and Kellomaki, 1982; Kuuluvainen and Pukkala, 1987; Peddle et al., 1995; Chen and Leblanc, 1997). For instance, conical- or cylindrical-shaped crowns typical of boreal conifers are generally narrow and tend to have a relatively high ratio of crown height to crown width. This results in a relatively small surface area of crown exposed to the upper canopy, and hence a lesser proportion of the shadow component is created by shadows from within and on the side of conical- or cylindrical-shaped crowns. On the other hand, spherical-shaped crowns that are typical of boreal deciduous species have a lower ratio of crown height to crown width. Consequently, a larger surface area of the crown is exposed in the upper canopy and a greater proportion of the shadow component is created within and on the side of crowns. Shadows within crowns and on the sides of crowns tend to be brighter than those created deeper in the canopy and adjacent to conifer species (Seed and King, 1997; 2001). Overall, from an image perspective, these physical differences in the light regime between conifer and deciduous species support the formation of different shadow brightness in imagery, with darker shadows generally associated with conifers and lighter shadows with deciduous trees (Leblon et al., 1996).

Accordingly, this research was designed to evaluate relations of shadow fraction and shadow brightness with  $LAI_e$  in a mixedwood boreal forest of variable canopy closure. Shadow information was derived from high spatial resolution airborne digital camera imagery capable of resolving the within-crown structure of individual trees. The off-nadir imaging capabilities of the digital camera system also afforded an appropriate situation to evaluate view-angle (combined optical and bidirectional reflectance distribution function or BRDF) effects on regression-based modelling of forest stand  $LAI_e$ .

## Objectives

The objectives of this research were to (i) examine and compare the relations of image shadow fraction and image

shadow brightness with  $LAI_e$ , both in reference to canopy closure; and (ii) evaluate the effect of view angle geometry on these relations. The focus of the research was not on development of predictive models for  $LAI_e$  or LAI, but on the inverse, i.e., how are variations in  $LAI_e$  manifested in shadow information in high-resolution imagery, and what are the impacts of canopy closure and view angle on shadow information? It was anticipated that the findings would aid in understanding the nature of image formation and structure in mixedwood forests and inform ongoing efforts in the research community in predictive modelling of LAI.

## Study site

The study site was located northwest of Timmins, Ontario, in a boreal forest situated in the Clay Belt region. It was a characteristically well-drained mixedwood uplands forest of the southern boreal region with a mainly deciduous overstory of trembling aspen (*P. tremuloides*) and balsam poplar (*P. balsamifera*), with some jack pine (*Pinus banksiana*) in the drier areas (Legasy et al., 1995). A mature conifer understory of white spruce (*P. glauca*) and balsam fir (*Abies balsamea*) was generally present in established sites, with the occasional black spruce (*P. mariana*) in wetter areas. Depending on successional stage and site factors, white spruce, black spruce, and balsam fir were also found in the overstory in varying proportions (Jones et al., 1983). An emergent shrub layer of alder (*Alnus* sp.) and hazelnut (*Corylus cornuta*) marked the more open canopies, with herbaceous layer abundance varying in association with local drainage patterns. The study area has been an ongoing site for research into modelling of localized stress from an adjacent mine site and development of forest structural condition monitoring methods using spectral, spatial, and radiometric fraction image measures extracted from digital camera imagery (Walsworth and King, 1999; Lévesque and King, 1999; 2002; Olthof and King, 2000).

## Methods

### Measurement of $LAI_e$ and canopy closure

Field data were collected in August 1996 from fifteen 20 × 20 m plots established along a 300 m transect in an area of mixedwood forest that had a visible range of species and stem density (see **Figure 1**). A complete census of trees greater than 2 m in height was conducted for diameter at breast height (DBH), species composition, height, and stem density. Effective leaf area index and canopy closure were both estimated indirectly for each study plot using the LAI-2000. Effective LAI was measured instead of LAI because in 1996 an optical instrument such as the TRAC (Chen and Cihlar, 1995) was not widely available and destructive or leaf trap collection methods were not feasible. The LAI-2000 contains fish-eye optics that transmit incident radiation onto five concentric rings sensitive to wavelengths between 320 and 490 nm. The function of the instrument is based on the assumption that radiation is strongly absorbed by vegetation in this region of the

spectrum, so the sensor should only see light (sky) and dark (canopy) regions needed to calculate the canopy gap fraction (Welles and Norman, 1991). The total field of view of the instrument is  $148^\circ$ , with rings centred at  $7^\circ$ ,  $22^\circ$ ,  $38^\circ$ ,  $52^\circ$ , and  $68^\circ$ ; however, any combination of rings can be masked in the final data analysis to restrict the sensor field of view. To calculate both mean  $LAI_c$  and canopy closure, the ratio of the above-canopy to below-canopy readings is required. The LAI-2000 was well suited to plot-based research given that the footprint of the instrument could be restricted and controlled, thus minimizing information collected outside plot boundaries.

Two LAI-2000 units were used to collect simultaneous above- and below-canopy readings with sample dates close to those of the airborne image acquisition. Above-canopy readings were taken adjacent to the transect from a unit set up in an open area that was large enough to not restrict the sensor's field of view. Below-canopy measurements were taken at flagged intervals 2 m above ground to avoid a dense shrub layer of alder (*Alnus* sp.) and hazelnut (*Corylus cornuta*) present in several plots. Three measurement points were located along the southern edge of the plots. Sample points were located 5, 10, and 15 m in from the east edge of the plot. An additional three sample points were located 10 m directly north of the first line of measurements, forming a sample grid of six points. At each measurement point, five separate readings were taken. In total, 30 LAI-2000 measurements were taken for each plot and the average of these readings was later used to calculate a mean  $LAI_c$  value for each plot. Of particular note, the sensor was always pointing into the plot to minimize the amount of canopy viewed outside the plots. As well, measurements were taken with the sun to the back of the operator at all times to prevent any possibility of intense light entering the sensor, even under homogeneously cloudy conditions (LI-COR, Inc., 1990). To minimize errors associated with the linear averaging of both gap and dense foliage, the azimuth field of view of the instrument was restricted to  $45^\circ$ . The fifth ring ( $68^\circ$ ) was masked during data analysis to decrease the field of view in the zenith direction and minimize inclusion of neighbouring trees outside the plot boundary (Dufrene and Breda, 1995). Again,

all readings were measured under uniform cloud cover to lessen potential errors from sunlit foliage (Welles and Norman, 1991). Lastly, the LAI-2000 units were calibrated against each other to correct for instrument bias. Canopy closure was derived from the first angle range (zenith angle  $0\text{--}15^\circ$ ) of the instrument such that canopy closure =  $[1 - P(7^\circ)] \times 100$  (Chen and Cihlar, 1996), where  $P(7^\circ)$  is the gap fraction from the first ring.

### Airborne imagery acquisition and processing

Images of the study plots were acquired at midday and under clear conditions in August 1996 using a Kodak DCS 420 colour infrared (CIR) camera. Originally developed for application within the United States Forest Service, these cameras were modified by the manufacturer to remove blue sensitivity and add near-infrared sensitivity to approximate the spectral range of Kodak 2443 CIR film; therefore the spectral bands were relatively wide, being approximately 100 nm, with significant spectral overlap (Bobbe and Zigadlo, 1995). The single charge-coupled device (CCD) used in the camera was sensitive to radiation between 400 and 1000 nm, but was filtered to provide spectral sensitivity between 500 and 800 nm (Eastman Kodak Company, 1996), with nominal bandwidth centres at 555 nm (green), 670 nm (red), and 760 nm (near infrared) (T. Birdsall, personal communication, 1997). The CCD produced three  $1524 \times 1012$ , 12-bit channels in the green, red, and near infrared through use of postprocessing colour estimation (interpolation) software. The data were converted to eight bit for analysis. The camera housing was a 35 mm Nikon camera body with a 28 mm focal length lens. The total angle of view along the principal plane was approximately  $28^\circ$ . Images were acquired with an approximate ground pixel spacing of 25 cm and 60% forward overlap.

Reference targets set up in the field every 20 m along the study transect, at several locations within the forest, and in several openings nearby were used as ground-control points to aid in locating plots in the imagery. Plot locations were identified in the imagery to an accuracy of less than two pixels, or approximately 50 cm. The elevation difference along the

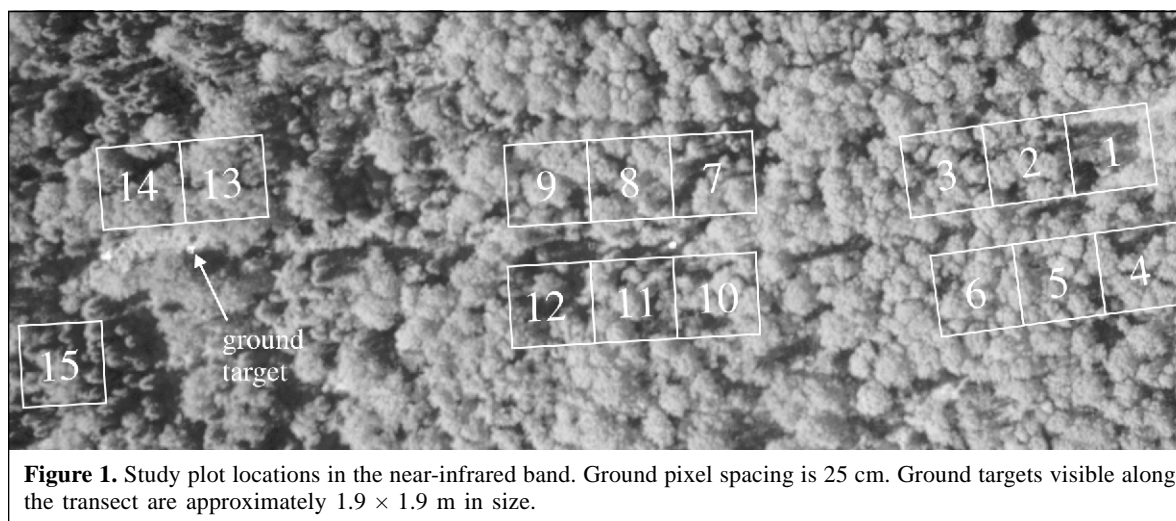


**Figure 1.** Study plot locations in the near-infrared band. Ground pixel spacing is 25 cm. Ground targets visible along the transect are approximately  $1.9 \times 1.9$  m in size.

transect was less than 1.5 m, therefore topographic correction was not necessary (Walsworth, 1997). Once the plots were located, image overlap of 60% allowed each plot to be cropped at three separate view angles, from a series of five overlapping images, resulting in a total of 45 subscenes ( $80 \times 80$  pixels each). The distance from the image centre to the centre pixel of each plot subscene was then determined to calculate the view zenith angle for each plot along the image principal plane. Plot position was also referenced in relation to the solar azimuth, which determines the scattering direction in the image. Plots in the backscattering zone (on the side of the image away from the sun) were assigned a positive view zenith angle, and plots in the forward-scattering zone (side of image towards the sun) were assigned a negative view zenith angle. Characterizing scattering direction was important because it was thought to be a strong determinant of image shadow component information (Gerard and North, 1997; Leblanc et al., 1997) and might influence the regression models developed with LAI<sub>e</sub>.

Spatial variations in brightness across the sensor field of view were evident in the airborne imagery and, as research suggests, were considered to have an effect on image feature extraction (King, 1992; Pellikka, 1996). In the forward-scattering zone, both bidirectional and optical effects combined to reduce image brightness, whereas in the backscattering zone bidirectional effects increased image brightness and vignetting progressively decreased image brightness. The net effect was still a darkening of the image in the backscattering zone, but less so than in the forward-scattering direction. It was evident that these combined view angle variations in image brightness could not be fully corrected. Instead, the analytical methods were adapted to minimize them (as described in the next section).

### Extraction of image shadow fraction and brightness

Image analysis was conducted on individual plot subscenes under the assumption that they were small enough ( $80 \times 80$  pixels) and would not be subject to within-plot variations because of optical or BRDF effects as discussed previously. However, plots located in different parts of the image had different average brightness because of these effects. To normalize average plot brightness, principal component analysis (PCA) was conducted. In PCA, a new set of rotated and orthogonal axes was generated through the linear combination of the original green, red, and near-infrared spectral bands. The largest total variance was mapped to the first component, with decreasing variance being mapped to successive components until the total image variance was mapped. Because PCA is a linear transformation, the rotation solution does not alter the structural information of the component histograms; it only shifts their brightness, which when applied locally on plot subscenes served to normalize scene brightness to a common midpoint (127.5 digital numbers (DN) in eight bit imagery) while maintaining the variance in shadow brightness associated with species composition. Applying PCA to local or subset areas of the image allowed

high-frequency details to be extracted, as any low-frequency noise such as optical effects and artefacts from CCD interpolation (Dean et al., 2000) are removed in the process. Given the wide and overlapping bands of the Kodak DCS 420 camera were highly correlated, PCA also provided reduced dimensionality without a loss of information. The variance accounted for by the first principal component (PC1) typically ranged from 95 to 98%, with the second component (PC2) containing between 2 and 4% of total image variance. The relatively equal and positive coefficients of the eigenvectors of the three original spectral bands suggested that PC1 contained brightness information that was common to all bands. Differences in the coefficients and their signs between the visible and near-infrared bands in PC2 suggested it contained information on image contrast; specifically, the edge between areas with high near-infrared and low visible band brightness. However, because a large proportion of the edge defined in PC2 did not visually correspond to the edge between component fractions, it was discarded. The third component (PC3) usually contained less than 1% of the total image variance and was interpreted as image noise. Only PC1 was used to extract the shadow information.

Scene fraction analysis in high-resolution digital camera imagery differs from methods using spectral mixture analysis of lower resolution imagery because individual scene fractions can be resolved, meaning it is not necessary to unmix individual pixels into their radiometric components. As a result, the image shadow fraction was extracted directly from the first principal component using a K-means clustering algorithm on the individual plots. K-means is an unsupervised classification method that iteratively assigns pixels to clusters by nearest neighbour principles (Jensen, 1996). The initial cluster centres were located diagonally along the  $n$ -dimensional histogram. Movement of the cluster means continued until the algorithm converged and cluster movement was less than 1% of all cluster means (PCI Geomatics Group Inc., 2001). From experience, the best segmentation tended to occur when a larger number of clusters, typically 8–12, were requested. The approach of initially having a large number of small clusters allowed greater flexibility in objectively defining the final shadow class and ensured no loss of information at the start. This was the primary advantage of using K-means to define the shadow fraction as opposed to visually dividing the histogram into shadow and nonshadow. Progressive signature merging of clusters then allowed class separation to be evaluated visually through overlay of bitmaps of the selected classes with the original images and statistically using transformed divergence. After review, the first four clusters from the K-means solution were merged and selected as the shadow class. The transformed divergence between this shadow class and the remaining pixels for data at nadir in the three scenes was between 1.9 and 2.0. This is considered to be very good separation (Jensen, 1996). Note that with such small pixel spacing, both within-crown and between-crown shadows were extracted. As a final step, the proportional area of the shadow fraction in each of the plot subscenes was recorded. Shadow fraction brightness for the

plot subscenes was then determined relative to the midpoint brightness of PC1 (i.e., shadow brightness = 127.5 – shadow brightness PC1).

### Linear regression analysis

Bivariate regression analysis was used to determine the relations between the image shadow fraction and  $LAI_e$  and between image shadow brightness and  $LAI_e$ . To determine the impact of canopy closure on the observed relations, the data were stratified into one of three canopy classes: (i) greater than 80% closure, (ii) 70–80% closure, and (iii) less than 70% closure. Cut points for the class intervals were selected to provide three equal-sized groups, with each group having the same number of cases. The effect of view geometry on the shadow– $LAI_e$  relations was also evaluated through further stratification. View zenith angle was used as a selection variable to limit the regression analysis to three subset groups that included (i) nadir (plots within  $\pm 3.5^\circ$  of the image centre), (ii) the forward-scattering direction (plots having a negative view zenith angle of  $-3.6^\circ$  to  $-14^\circ$ ), and (iii) the backscattering direction (plots having a positive view zenith angle of  $+3.6^\circ$  to  $+14^\circ$ ). Again, the view zenith angle geometry is relative to the image principal plane and solar azimuth position. **Table 1** summarizes the angular information for each of the data sets used in the regression analysis. For all regression analysis,  $LAI_e$  was entered as the independent variable and the image measures were entered as the dependent variable. The intention was to analyze effects of  $LAI_e$  on image shadow information under varying closure and view angle and not to predict  $LAI_e$  (where it would have been the dependent variable).

**Table 1.** Summary of angular information for data sets used in regression analysis.

Scattering direction	View angle ( $^\circ$ )			SD
	Mean	Min.	Max.	
Nadir (n)	+1.0	0.0	+3.5	1.9
Forward (f)	-7.3	-3.6	-13.1	2.7
Back (b)	+6.4	+3.6	+12.3	2.6

Note: SD, standard deviation.

## Results

### Trends in $LAI_e$ and canopy cover

Overall,  $LAI_e$  ranged from 1.12 to 4.92, the highest values occurring in areas with a mature conifer understory as seen in plots 7, 8, and 12–15 (**Table 2**). The lowest values were seen in plots 1 and 2, where closure was relatively low and contribution from the understory was minimal. These observed differences and other similarities (e.g., plots 7 and 8) were most likely attributed to differences in species composition within the plots rather than differences in tree size or stem density. For example, the higher than average  $LAI_e$  values observed in plots 7, 8, and 12–15 are coupled with a relatively high percent composition of conifer species and lower percent composition of deciduous species. There was also a distinct trend of lower than average  $LAI_e$  associated with a higher than average composition of trembling aspen in plots 1–6. Accordingly, correlation analysis revealed significant negative relations ( $r = -0.76$ ;  $p = 0.001$ ) between  $LAI_e$  and percent deciduous composition and a significant positive correlation ( $r = 0.63$ ;  $p = 0.05$ ) between  $LAI_e$  and percent composition of conifers. These results make apparent the importance of species composition in determining

**Table 2.** Summary of forest structure and composition for the 15 study plots.

Plot No.	$LAI_e$	Canopy closure (%)	Basal area ( $m^2/ha$ )	Density (stems/ha)	Mean DBH (cm)	Relative composition	
						Total conifer	Total deciduous
1	1.12	26	2.3	125	34.9	0.20	0.80
2	1.59	67	13.6	600	17.6	0.67	0.33
3	2.18	70	36.5	1075	16.1	0.67	0.33
4	1.88	73	15.1	525	19.4	0.61	0.39
5	2.13	68	14.5	525	20.8	0.62	0.38
6	2.69	67	54.4	1075	19.7	0.56	0.44
7	3.30	73	32.0	1050	15.4	0.76	0.24
8	3.40	70	16.0	625	18.3	0.88	0.12
9	2.72	79	38.3	800	22.2	0.59	0.41
10	2.90	48	7.8	350	22.9	0.57	0.43
11	2.58	76	35.2	650	26.2	0.24	0.76
12	3.98	89	56.6	1125	18.5	0.67	0.33
13	3.36	87	76.7	1950	12.7	0.79	0.21
14	3.53	91	40.2	850	21.1	0.74	0.26
15	4.92	95	53.0	1075	19.1	0.93	0.07
Mean	2.82	72	32.7	825	20.2	0.63	0.37

LAI<sub>e</sub> and the need to account for these variations if LAI<sub>e</sub> is to be successfully estimated using remote sensing techniques.

The range of canopy closure along the transect was 68%. Maximum closure was measured in plots with a mixed overstory of white spruce and trembling aspen where values approached 95%. In contrast, open canopies were typically single-layer forest with no understory, such as plot 1 with a closure of 26%. Of note, there was also a significant, but not very strong, association between LAI<sub>e</sub> and canopy closure ( $r = 0.73$ ;  $p = 0.002$ ), as they were both derived from the same instrument. However, canopy closure tended to be more variable and dependent on instrument position than was LAI<sub>e</sub> because it was calculated from a single zenith angle ranging from 0° to 15° rather than integrated over the full hemisphere of the LAI-2000 (Chen et al., 1999). Regardless, canopy closure provided estimates on the percent vegetation cover from a vertical view, therefore it is a unique statistical measure of the amount of open space or gaps within and between crowns and may have an effect on the shadow fraction.

### Relations of shadow fraction with LAI<sub>e</sub>

Figure 2 shows that relations between the shadow fraction and LAI<sub>e</sub> were clearest at nadir and in the backscattering direction, when the coefficient of determination ( $r^2$ ) was greatest and maximum variation in the shadow fraction among

plots was accounted for. Although relations were weak, the similar model fit and significance at nadir and in the backscattering direction suggest the effect of view geometry on the shadow fraction and LAI<sub>e</sub> relationship is minimal in the backscattering direction for this study. In contrast, there were no linear relations between shadow fraction and LAI<sub>e</sub> in the forward-scattering direction. Because view angle effects in the forward-scattering direction result in a greater probability of the sensor observing shadows compared to either nadir or the backscattering direction (i.e., shadow fraction was generally greater in the forward-scattering direction for all plots), there was a significantly different model fit for the forward direction. Specifically, the y intercept in the forward-scattering direction was greater and the slope of the regression line was flat as compared with the y intercept and slope at nadir and in the backscattering direction.

The considerable scatter observed in the relations at all view geometries was attributed to differences in canopy closure, as shown in Figure 2. For example, with canopy closure less than 70% (data points denoted by l, low closure, in Figure 2) there was a negative trend in shadow fraction associated with increasing LAI<sub>e</sub> ( $r^2 = 0.67$  at nadir), but at canopy closure between 70 and 80% (data points denoted by m, moderate closure, in Figure 2) there were no clear linear trends present with LAI<sub>e</sub>. Where canopy closure was greater than 80% (data points denoted by h, high closure, in Figure 2), a positive trend

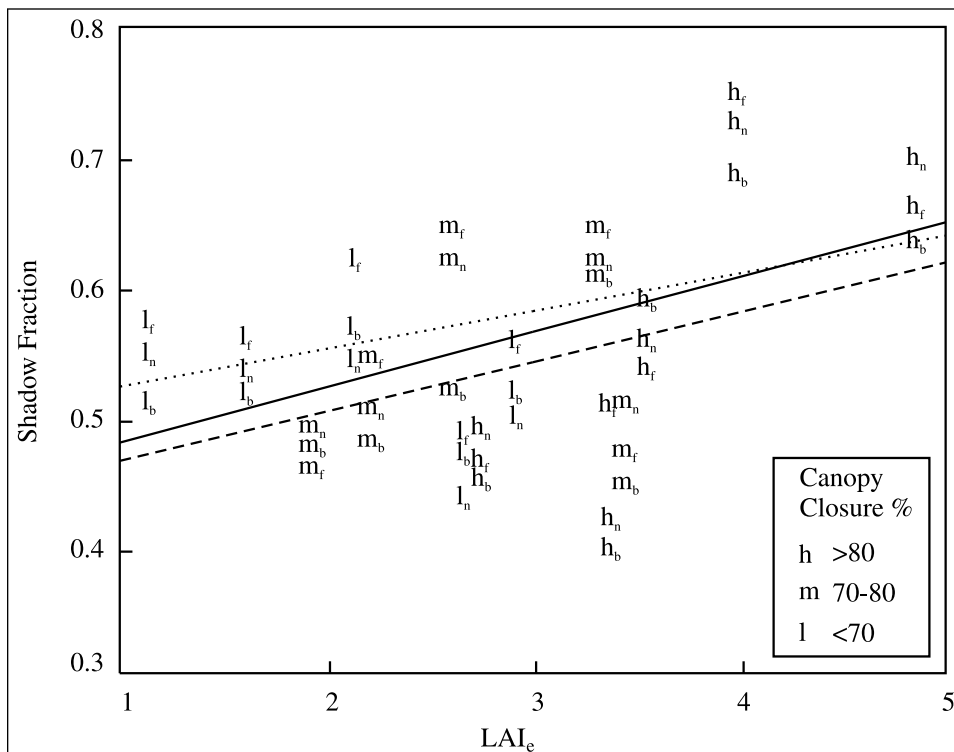


**Figure 2.** Scatter plot of shadow fraction and LAI<sub>e</sub>. Separate relations are derived for nadir and forward-scattering and backscattering directions. Data points are stratified with canopy closure, which is classified as low (l), moderate (m), and high (h), with subscripts n, b, and f indicating at nadir and in the backscattering and forward-scattering directions, respectively. For nadir (solid line),  $r^2 = 0.24$  and  $p = 0.068$ ; for forward-scattering direction (dotted line),  $r^2 = 0.12$  and  $p = 0.211$ ; and for backscattering direction (broken line),  $r^2 = 0.23$  and  $p = 0.074$ .

between the shadow fraction and  $LAI_e$  ( $r^2 = 0.77$  at nadir) was evident. The observed scatter in these relations suggests that the shadow fraction is not very sensitive to changes in  $LAI_e$  at low to medium closure, but that sensitivity to changes in  $LAI_e$  increases at closure greater than 80%. In response to these observations, a secondary analysis using curvilinear (quadratic) regression showed some improvement in fit for the nadir view regression model, that is,  $r^2$  improved to 0.43 with a significance of 0.034. Still, curvilinear regressions for the backscattering and forward-scattering directions were less significant than linear models already described here, signifying no overall improvements in using nonlinear regression to describe the shadow fraction –  $LAI_e$  relationship.

### Relations of shadow brightness with $LAI_e$

Bivariate regression of shadow brightness and  $LAI_e$  (Figure 3) produced significantly improved results over those with shadow fraction. A negative trend was evident between shadow brightness and  $LAI_e$  across the full range of canopy closure. The clearest relations were at nadir and in the backscattering direction, with both regressions having a similar fit and significance. Even relations in the forward-scattering direction were significant. The main reason for the improvement was the decrease in scatter caused by study plots with canopy closure less than 80%, which generally confounded the shadow

fraction –  $LAI_e$  relationship. Although shadow brightness was still in part dependent on canopy closure, this dependency was linear in nature, that is, higher closure resulted in decreased shadow brightness and lower canopy closure resulted in increased shadow brightness (Seed and King, 2001). For this reason, the relations between  $LAI_e$  and shadow brightness remained linear despite variations in canopy closure.

The slopes of all three regression lines were approximately equal. All plots generally showed a consistent shift in shadow brightness with changing view geometry. In the forward-scattering direction, however, there was a noticeable decrease in the average shadow brightness, that is, the intercept for the forward-scattering direction was shifted down ( $y = 38.5$ ) relative to nadir. This indicated that shadows were generally darker and dependent on view zenith angle in the forward-scattering direction. This dependency on view zenith angle was presumably because of residual optical and bidirectional effects on the image. For example, as the shaded sides of crowns were revealed in the forward-scattering direction, a greater proportion of darker shadows on the undersides of crowns may have been visible to the sensor, resulting in decreased shadow brightness.

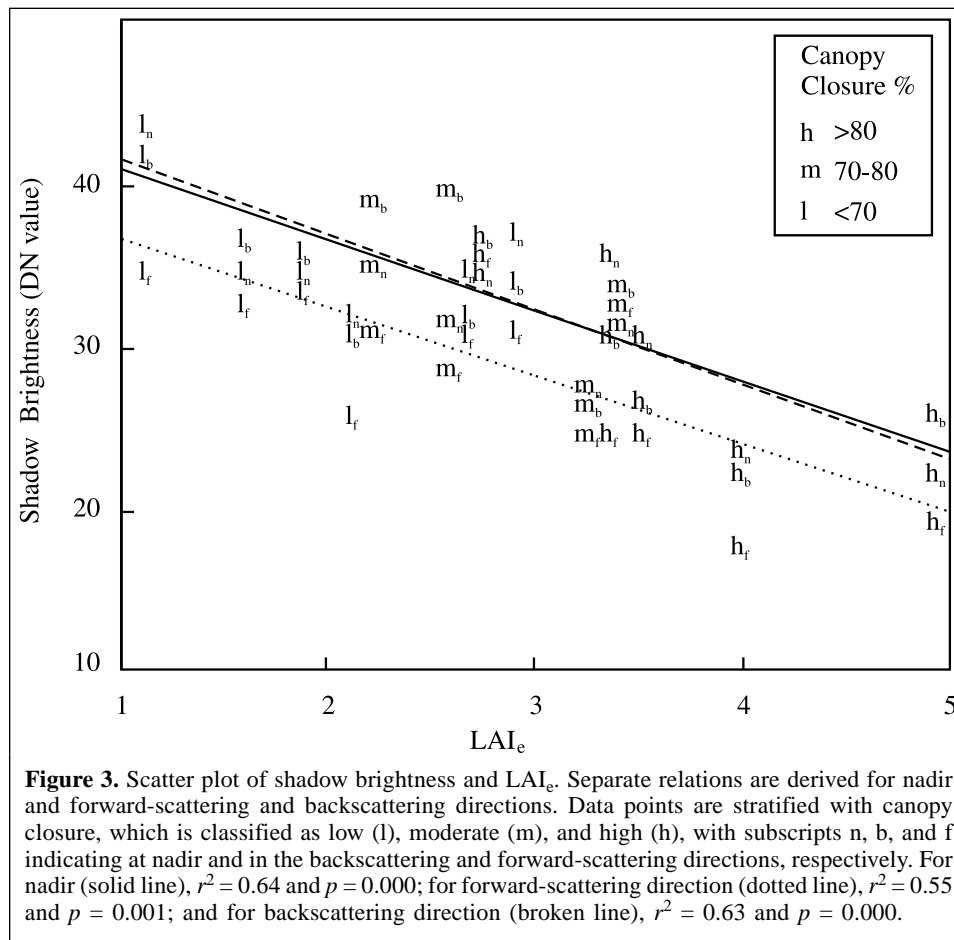


**Figure 3.** Scatter plot of shadow brightness and  $LAI_e$ . Separate relations are derived for nadir and forward-scattering and backscattering directions. Data points are stratified with canopy closure, which is classified as low (l), moderate (m), and high (h), with subscripts n, b, and f indicating at nadir and in the backscattering and forward-scattering directions, respectively. For nadir (solid line),  $r^2 = 0.64$  and  $p = 0.000$ ; for forward-scattering direction (dotted line),  $r^2 = 0.55$  and  $p = 0.001$ ; and for backscattering direction (broken line),  $r^2 = 0.63$  and  $p = 0.000$ .

## Discussion

Although the wide-band CIR imagery used in this study did not provide the spectral precision or information content of advanced multispectral sensors, the additional spatial information allowed individual radiometric fractions to be seen and, in turn, provided greater precision in defining and extracting shadow information.

The observed relations between shadow fraction and  $LAI_e$  were somewhat unexpected given the strength of previous research in applying the shadow fraction for the estimation of LAI in homogeneous forest stands (Hall et al., 1996; Peddle et al., 2001). Although direct comparisons are not possible, the nature of the results presented here suggests that the shadow fraction may not be optimal for use in the estimation of  $LAI_e$  in boreal mixedwood forest. For stands with low to medium closure, the gap size and the number of gaps in the forest are important physical controls over the amount of shaded background observed by the sensor and may in part explain the poor relations shown in this research. In general, the shadow fraction will be greater in forest that has either large numbers of small gaps or in forest with few but large gaps. When occurring together in the same stand, these two cases will confound the shadow fraction –  $LAI_e$  relationship because plots with unique  $LAI_e$  values may have a similar shadow fraction, but with different physical reasons controlling that shadow fraction. For example, plot 1, having low closure, low  $LAI_e$ , and a shadow fraction of 0.55, was characterized by a single large gap visible at nadir, whereas plot 14, with high closure, high  $LAI_e$ , and a shadow fraction of 0.56, had a large number of smaller gaps visible at nadir. This represents a 1% difference in shadow fraction between plots that were separated by  $LAI_e$  of 2.41. These differences emphasize that gap size and frequency are important factors in determining shadow fraction. Again, the complex canopy architecture of mixedwood forest is quite different from the density-dependent nature of homogeneous conifer stands such as black spruce, where Hall et al. (1995) found strong relations between LAI and shadow fraction. The added uncertainty from several vertical strata often found in mixedwood forest requires further empirical and, in particular, theoretical investigation as to their effects on image radiometric structure. Alternatively, if measured over a wider view angle, these variations in the shadow component have potential for providing additional information to improve prediction of  $LAI_e$  and LAI through BRDF modelling.

Results from this research also indicate that the hypothesized link between the brightness of shadows cast by tree crowns and the light regime in mixedwood forest was supported by the empirical relationship presented in this paper. Shadow brightness was strongly related to  $LAI_e$  because it was not adversely affected by canopy closure while remaining sensitive to species composition. In other words, shadow brightness was less dependent on gap arrangement and size and, as such, was more consistent with view angle than was shadow fraction. For example, shadow brightness at nadir had a digital number of 44 in plot 1 and 31 in plot 14. This represented a difference of

approximately 30% in the shadow brightness and offers reason for the effectiveness of shadow brightness in assessing overstory  $LAI_e$ . These findings demonstrate the potential of shadow brightness to effectively unify canopies with different cover types and cover amount for empirical modelling of  $LAI_e$ .

In general, the physical links between shadow brightness and the light transmission of conifer and deciduous crowns support a linear relationship with  $LAI_e$ ; however, there was still room for improvement. Certainly, some of the observed data point scatter in this relationship was caused by the surface onto which the shadows were cast, meaning that canopy understory effects were still influencing the shadow brightness –  $LAI_e$  relationship (Leblon et al., 1996; Seed and King, 2001). Separation of the understory and overstory effects on shadow brightness would be difficult, but an additional measurement of the standard deviation of shadow brightness or the grey-level co-occurrence texture of shadow might be able to capture the tonal variations within the shadow component that are associated with understory trees. Current research in temperate hardwood forest is attempting to do this by measuring  $LAI_e$  at various heights in the canopy to construct a vertical  $LAI_e$  profile for differentiating understory and overstory contributions to shadow information.

From the associated analysis of the effects of view geometry it was apparent that even with the relatively narrow total angle of view along the principal plane, combined optical-BRDF variations affected the  $LAI_e$ –shadow relations. The possibility of normalizing the off-nadir shadow fraction and shadow brightness to nadir is something that may deserve investigation in future research. Because of difficulties associated with correcting these and other optical effects operationally, however, it may be preferable to isolate regression analysis to nadir and the backscattering zone. Although attempts to correct image optical effects have shown moderate success (e.g., Pellikka, 1996), bidirectional reflectance variations are a result of geometric changes in the image scene and thus are more difficult to correct. An operationally feasible alternative would be to apply methods such as the local PCA and K-means analysis used in this research to minimize these reflectance variations. Similarly, when building an image mosaic using digital camera imagery with sufficient forward overlap, imagery in the forward-scattering zone can be discarded in favour of imagery in the backscattering zone and nadir (in this research approximately  $-4^\circ$  to  $+14^\circ$ ). Overall, view angle geometry does influence  $LAI_e$  – shadow component relationships and cannot be ignored, especially if regression models are applied over wide spatial scales or time frames.

Lastly, as a means of evaluating the potential of the shadow information for predictive modelling, multiple regression analyses were performed on the nadir dataset. Results from two variable regression analyses with  $LAI_e$  as the dependent variable and shadow fraction and shadow brightness entered as the independent variables (adjusted  $R^2 = 0.61$ ;  $p = 0.001$  at nadir) showed no significant improvement in the relationship with  $LAI_e$  when shadow brightness was used alone. This indicated that no additional information was provided in

coupling shadow fraction and shadow brightness for describing the observed variations in  $LAI_c$ .

It is acknowledged that, although the spatial scale used in this study was sufficient for extracting information on both shadow brightness and shadow fraction, future research should focus on scaling up shadow information to coarser resolutions to determine an efficient spatial scale for application to large-area study sites. The methods presented are appropriate for application with high-resolution imagery but are expected to be difficult to apply with coarse-scale imagery not capable of resolving radiometric elements within individual tree crowns.

Future research will also include larger sample sizes and validation in forests with a wider range of LAI as opposed to  $LAI_c$ . Because the LAI-2000 instrument assumes a random distribution of foliage elements and this assumption is generally violated in natural forest where vegetation can be clumped, the LAI-2000 did not provide a true measure of canopy leaf area. Accordingly, consideration of a foliage shoot clumping index would improve the optical measures of LAI, providing values closer to the true canopy LAI (Chen and Cihlar, 1995). For temporal studies involving the monitoring of same-site or local-scale environmental problems, however,  $LAI_c$  is considered a good predictor of the radiation intercepted by the forest canopy. As an easily obtained measure of the radiation interception of the canopy, it is also temporally less variable than LAI and has been recommended by Chen and Cihlar (1996) as a basic operational measure of stand structure.

## Conclusions

This research contributes to improving our understanding of the physical and technical mechanisms responsible for the relationship between  $LAI_c$  and airborne-derived image shadow information in boreal mixedwood forest. Specifically, this research draws the following conclusions:

- (1) Linear relations between shadow brightness and  $LAI_c$  were negative and significant for all view geometries. Dependency on canopy closure was linear. The sensitivity of shadow brightness to the light regime of conifer and deciduous crowns might allow for species-independent models in the estimation of  $LAI_c$  in boreal mixedwood forest.
- (2) Linear relations between shadow fraction and  $LAI_c$  were positive but insignificant for all view geometries because the shadow fraction was not sensitive to changes in  $LAI_c$  below 80% closure. Although relations were linear in stands with closure greater than 80%, overall a nonlinear dependency on closure may limit application of the shadow fraction for  $LAI_c$  estimation in forests with complex canopy architecture.
- (3) Relations between both types of shadow information and  $LAI_c$  were strongest at nadir and in the backscattering direction. In future, models should be preferentially developed and applied to these areas. The effects of view

geometry on shadow brightness were consistent for all scattering directions, although residual image bidirectional and optical effects in the forward-scattering direction influenced them. The effects of view geometry on the shadow fraction were not consistent for all scattering directions and were more likely influenced from associated changes in image view geometry.

Currently, in the application of image structure analysis to high-resolution imagery, only spectral information is used in defining the radiometric components, but as conceptualized by Seed and King (1997) and verified by Peddle and Johnson (2000), the potential to define image components by their spectral and spatial position in the forest canopy does exist. Future research will continue to pursue methods to better integrate spatial information into the classification process as suggested by Cihlar et al. (2000). Investigation of the spatial relationships between image shadow and sunlit components including adjacency and the spatial co-occurrence of scene components in high spatial resolution imagery will also be pursued. Lastly, additional image structural measures such as component shape, perimeter, and frequency will be explored for their potential to provide surrogate information on  $LAI_c$  and vertical  $LAI_c$  in temperate deciduous forest.

## Acknowledgements

Research for this study was funded through a Natural Sciences and Engineering Research Council of Canada grant to D. King. Carleton University and the Canada Centre for Remote Sensing provided additional support for data acquisition. Kodak Inc. of Rochester, New York, provided the Kodak DCS 420 CIR camera on loan. Access to the study site was granted with permission of Falconbridge Inc. of Timmins, Ontario.

## References

- Bobbe, T.J., and Zigadlo, J.P. 1995. Color infrared digital camera systems use for natural resources aerial surveys. *Earth Observation Magazine*, Vol. 4, No. 6, pp. 60–62.
- Bonan, G.B., and Shugart, H.H. 1989. Environmental factors and ecological processes in boreal forests. *Annual Review of Ecological Systems*, Vol. 20, pp. 1–28.
- Brown, L., Chen, J.M., Leblanc, S.G., and Cihlar, J. 2000. A shortwave infrared modification to the simple ratio for LAI retrieval in boreal forests: an image and model analysis. *Remote Sensing of Environment*, Vol. 71, pp. 16–25.
- Chen, J.M., and Cihlar, J. 1995. Plant canopy gap-size analysis theory for improving optical measurements of leaf area index. *Applied Optics*, Vol. 34, No. 27, pp. 6211–6222.
- Chen, J.M., and Cihlar, J. 1996. Retrieving leaf area index of boreal conifer boreal forest using Landsat TM images. *Remote Sensing of Environment*, Vol. 55, pp. 153–162.

- Chen, J.M., and Leblanc, S.G. 1997. A four-scale bidirectional reflectance model based on canopy architecture. *IEEE Transactions on Geoscience and Remote Sensing*, Vol. 35, No. 5, pp. 1316–1337.
- Chen, J.M., Leblanc, S.G., Miller, J.R., Freemantle, J., Loechel, S.E., Walthall, C.L., Innanen, K.A., and White, H.P. 1999. Compact airborne spectrographic imager (CASI) used for mapping biophysical parameters of boreal forests. *Journal of Geophysical Research*, Vol. 104, No. D22, pp. 27 945 – 27 958.
- Cihlar, J., Latifovic, R., and Beaubien, J. 2000. A comparison of clustering strategies for unsupervised classification. *Canadian Journal of Remote Sensing*, Vol. 26, No. 5, pp. 446–454.
- Constabel, A.J. 1995. *Light transmission through boreal mixedwood stands*. M.Sc. thesis, University of Alberta, Edmonton, Alta.
- Constabel, A.J., and Liefvers, V.J. 1996. Seasonal patterns of light transmission through boreal mixedwood canopies. *Canadian Journal of Forest Research*, Vol. 26, pp. 1008–1014.
- Danson, M.F., and Curran, P.J. 1993. Factors affecting the remotely sensed response of coniferous forest plantations. *Remote Sensing of Environment*, Vol. 43, pp. 55–65.
- Dean, C., Warner, T.A., and McGraw, J.B. 2000. Suitability of the DCS460c colour digital camera for quantitative remote sensing analysis of vegetation. *Journal of Photogrammetry and Remote Sensing*, Vol. 55, pp. 105–118.
- Dufrene, E., and Breda, N. 1995. Estimation of deciduous forest leaf area index using direct and indirect methods. *Oecologia*, Vol. 104, pp. 156–162.
- Eastman Kodak Company. 1996. *Preliminary product description and specifications: KODAK digital color infrared camera*. Aerial Systems, Eastman Kodak Company, Rochester, N.Y.
- Ekstrand, S. 1994. Assessment of forest damage with Landsat TM: correction of varying forest stand characteristics. *Remote Sensing of Environment*, Vol. 47, pp. 291–302.
- Franklin, J., Davis, F.W., and Lefebvre, P. 1991. Thematic mapper analysis of tree cover in semiarid woodlands using a model of canopy shadowing. *Remote Sensing of Environment*, Vol. 36, pp. 189–202.
- Gastellu-Etchegorry, J.P., Demarez, V., Pinel, V., and Zagolski, F. 1996. Modeling radiative transfer in heterogenous 3-D vegetation canopies. *Remote Sensing of Environment*, Vol. 58, pp. 131–156.
- Gerard, F.F., and North, P.R.J. 1997. Analyzing the effects of structural variability and canopy gaps on forest BRDF using a geometrical-optical model. *Remote Sensing of Environment*, Vol. 62, pp. 46–62.
- Hall, F.G., Shimabukuro, Y.E., and Huemmrich, K.F. 1995. Remote sensing of forest biophysical structure using mixture decomposition and geometric reflectance models. *Ecological Applications*, Vol. 5, No. 4, pp. 993–1013.
- Hall, F.G., Peddle, D.R., and LeDrew, E.F. 1996. Remote sensing of biophysical variables in boreal forest stands of *Picea mariana*. *International Journal of Remote Sensing*, Vol. 17, No. 5, pp. 3077–3081.
- Haralick, R.M., Shanmugam, K., and Dinstein, I. 1973. Textural features for image classification. *IEEE Transactions on Systems, Man, and Cybernetics*, Vol. 3, pp. 610–621.
- Jensen, J.R. 1996. *Introductory digital image processing: a remote sensing perspective*. Prentice Hall, Toronto.
- Jones, R.K., Pierpoint, G., Wickware, G.M., Jeglum, J.K., Arnup, R.W., and Bowles, J.M. 1983. *Field guide to forest ecosystem classification for the clay belt, site region 3e*. Ontario Ministry of Natural Resources, Toronto, Ont.
- King, D.J. 1992. Evaluation of radiometric quality, statistical characteristics and spatial resolution of multispectral videography. *Journal of Imaging Science and Technology*, Vol. 36, pp. 394–404.
- Kneeshaw, D.D., and Bergeron, Y. 1998. Canopy gap characteristics and tree replacement in the southeastern boreal forest. *Ecology*, Vol. 79, No. 3, pp. 783–794.
- Kuuluvainen, T., and Pukkala, T. 1987. Effect of crown shape and tree distribution on the spatial distribution of shade. *Agricultural and Forest Meteorology*, Vol. 40, pp. 215–231.
- Leblanc, S.G., Chen, J.M., and Cihlar, J. 1997. Directionality of NDVI in boreal forests: a model interpretation of measurements. *Canadian Journal of Remote Sensing*, Vol. 23, pp. 369–380.
- Leblon, B., Gallant, L., and Granberg, H. 1996. Effects of shadowing types on ground-measured visible and near-infrared shadow reflectances. *Remote Sensing of Environment*, Vol. 58, pp. 322–328.
- Legacy, K., Beadman-LaBelle, S., and Chambers, B. 1995. *Forest plants of northeastern Ontario*. Lone Star Press, Edmonton, Alta.
- Lévesque, J., and King, D.J. 1999. Airborne digital camera image semivariance for evaluation of forest structural damage at an acid mine tailings site. *Remote Sensing of Environment*, Vol. 68, pp. 112–124.
- Lévesque, J., and King, D.J. 2003. Spatial analysis of radiometric fractions from high-resolution multispectral imagery for modelling forest structure and health. *Remote Sensing of Environment*. In press.
- Li X., and Strahler, A.H. 1985. Geometric-optical modeling of a conifer forest canopy. *IEEE Transactions on Geoscience and Remote Sensing*, Vol. 23, pp. 705–721.
- LI-COR, Inc. 1990. *LAI-2000 plant canopy analyzer operating manual*. LI-COR, Inc., Lincoln Nebr.
- Liefvers, V.J., Messier, C., Stadt, K.J., Gendron, F., and Comeau, P.G. 1999. Predicting and managing light in the understorey of boreal forests. *Canadian Journal of Forest Research*, Vol. 29, pp. 796–811.
- Oker-Blom, P., and Kellomaki, S. 1982. Theoretical computations of the role of crown shape in the absorption of light by forest trees. *Mathematical Biosciences*, Vol. 59, pp. 291–311.
- Oker-Blom, P., and Kellomaki, S. 1983. Effect of grouping of foliage on the within-stand and within-crown light regime: comparison of random and grouping canopy models. *Agricultural and Forest Meteorology*, Vol. 28, pp. 143–155.
- Olthof, I., and King, D.J. 2000. Development of a forest health index using multispectral airborne digital camera imagery. *Canadian Journal of Remote Sensing*, Vol. 26, No. 3, pp. 166–176.
- PCI Geomatics Group Inc. 2001. *PCI Geomatica software package, version 8.0*. PCI Geomatics Group Inc., Richmond Hill, Ont.
- Peddle, D.R., and Johnson, R.L. 2000. Spectral mixture analysis of airborne remote sensing imagery for improved prediction of leaf area index in mountainous terrain, Kananaskis, Alberta. *Canadian Journal of Remote Sensing*, Vol. 26, No. 3, pp. 177–188.
- Peddle, D.R., Hall, F.G., and LeDrew, E. 1995. Spectral mixture analysis and geometric-optical reflectance modeling of boreal forest biophysical structure: Superior National Forest, Minnesota. In *Proceedings of the 17th Canadian Symposium on Remote Sensing*, 13–17 June 1995, Saskatoon,

- Sask. Canadian Aeronautics and Space Institute, Ottawa, Ont. Vol. 2, pp. 617–622.
- Peddle, D.R., Hall, F.G., LeDrew, E.F., and Knapp, D.E. 1997. Classification of forest land cover in BOREAS II: comparison of results from a sub-pixel scale physical modeling approach and training based method. *Canadian Journal of Remote Sensing*, Vol. 23, No. 3, pp. 288–297.
- Peddle, D.R., Brunke, S.P., and Hall, F.G. 2001. A comparison of spectral mixture analysis and ten vegetation indices for estimating boreal forest biophysical information from airborne data. *Canadian Journal of Remote Sensing*, Vol. 27, No. 6, pp. 627–635.
- Pellikka, P. 1996. Illumination compensation for aerial video images to increase land cover classification accuracy in mountains. *Canadian Journal of Remote Sensing*, Vol. 12, pp. 368–381.
- Ranson, K.J., and Daughtry, S.T. 1987. Scene shadow effects on multispectral response. *IEEE Transactions on Geoscience and Remote Sensing*, Vol. 25, No. 4, pp. 502–509.
- Rosema, A., Verhoef, W., Noorbergen, H., and Borgesius, J. 1992. A new forest light interaction model in support of forest monitoring. *Remote Sensing of Environment*, Vol. 42, pp. 23–41.
- Ross, J. 1981. *The radiation regime and architecture of plant stands*. Dr. W. Junk Publishing, The Hague, The Netherlands.
- Seed, E.D., and King, D.J. 1997. Determination of mixed boreal forest stand biophysical structure using large scale airborne digital camera imagery. In *Proceedings of GER '97 – 19th Canadian Symposium on Remote Sensing*, 26–29 May 1997, Ottawa, Ont. Natural Resources Canada. CD-ROM, article 75, 8 pp.
- Seed, E.D., and King, D.J. 2001. Effects of stand overstory and understory structure on image shadow type in mixedwood boreal forest. In *Proceedings of the 18th Biennial Workshop on Color Photography and Videography in Resource Assessment*, 16–18 May 2001, Amherst, Mass. CD-ROM. American Society of Photogrammetry and Remote Sensing, Bethesda, Md.
- Spanner, M.A., Pierce, L.L., Peterson, D.L., and Running, S.W. 1990. Remote sensing temperate coniferous forest leaf area index. The influence of canopy closure, understory and background reflectance. *International Journal of Remote Sensing*, Vol. 11, No. 1, pp. 95–111.
- Stenberg, P., Kuuluvainen, T., Kellomaki, S., Grace, J.C., Jokela, E.J., and Gholz, H.L. 1994. Crown structure, light interception and productivity of pine trees and stands. *Ecological Bulletins*, Vol. 43, pp. 20–34.
- Walsworth, N.A. 1997. *Geographic image modeling of environmental degradation associated with acid mine drainage — KamKotia mine tailings*. M.A. thesis, Carleton University, Ottawa, Ont.
- Walsworth, N.A., and King, D.J. 1999. Image modelling of forest changes associated with acid mine drainage. *Computers and Geosciences*, Vol. 25, pp. 567–580.
- Welles, J.M., and Norman, J.M. 1991. Instrument for indirect measurement of canopy architecture. *Agronomy Journal*, Vol. 83, pp. 818–825.
- Wulder, M.A., LeDrew, E.F., Franklin, S.E., and Lavigne, M.B. 1998. Aerial image texture information in the estimation of northern deciduous and mixed wood forest leaf area index (LAI). *Remote Sensing of Environment*, Vol. 64, pp. 64–76.